Catal Lett (2016) 146:2173–2184
DOI 10.1007/s10562-016-1843-1

Estimation of Average Crystallites Size of Active Phase in Ceria-Supported Cobalt-Based Catalysts by Hydrogen Chemisorption vs TEM and XRD Methods

Grzegorz Słowik[1] · Anna Gawryszuk-Rżysko[2] · Magdalena Greluk[1] · Andrzej Machocki[1]

Received: 10 June 2016 / Accepted: 5 August 2016 / Published online: 18 August 2016

Abstract Cobalt catalysts with CeO_2 support, unpromoted and promoted with potassium were prepared by an impregnation method. Reduced catalysts were subjected to hydrogen chemisorption at different temperatures in the range of 313–453 K. Studies have shown that calculated Co crystallites size depends on the temperature of chemisorption. The average of size crystallites of the Co active phase obtained from the total and strong chemisorption data were compared with those from measurements by other techniques, TEM and XRD. The results of comparison allowed us to indicate the most suitable chemisorption temperature, different for unpromoted (383 K) and potassium-promoted (413 K) catalysts to determine the proper Co crystallites size of active phase, compatible with the crystallites size determined by the most objective method, i.e. by TEM measurements. In the case of small metal crystallites of active phase (4–5 nm) the divergence of their average size determined by hydrogen chemisorption and TEM methods and particularly by the XRD method is definitely higher than that in the case of larger crystallites (~12 nm).

Graphical Abstract

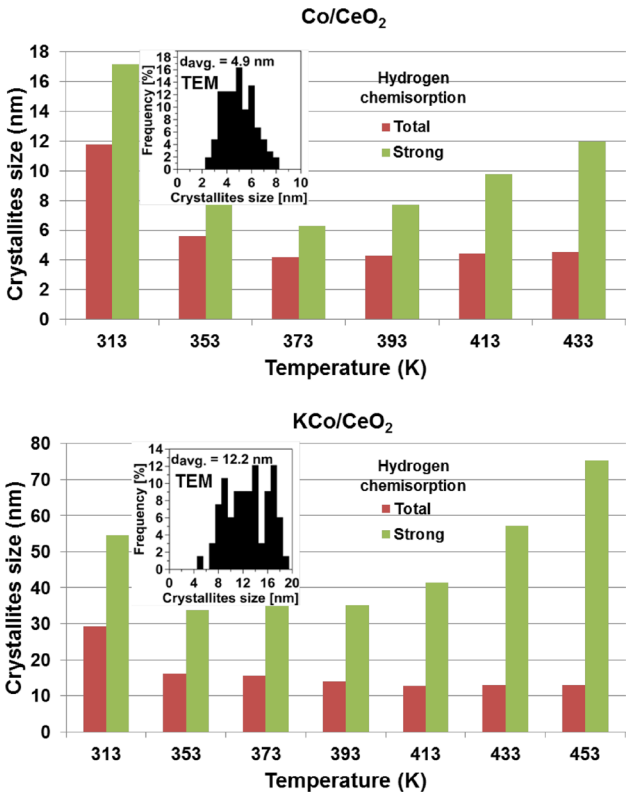

Keywords Heterogeneous catalysis · Electron microscopy · Nanostructure · Crystallites size · Hydrogen chemisorption · XRD · Cobalt-based catalysts

Electronic Supplementary Material The online version of this article (doi:10.1007/s10562-016-1843-1) contains supplementary material, which is available to authorized users.

✉ Grzegorz Słowik
Grzegorz.Slowik@poczta.umcs.lublin.pl

[1] Department of Chemical Technology, Faculty of Chemistry, University of Maria Curie-Sklodowska, 3 Maria Curie-Sklodowska Square, 20-031 Lublin, Poland

[2] Faculty of Chemistry, Analytical Laboratory, University of Maria Curie-Sklodowska, Lublin, Poland

1 Introduction

Heterogeneous catalysts through their irreplaceable role in chemicals and fuels production constitute a high interest research topic [1]. In such catalytic processes as the steam reforming of ethanol (SRE) [2] or the Fischer–Tropsch synthesis (FTS) [3, 4], besides operating conditions, the use of suitable catalyst plays a crucial role in achieving selective, efficient and economically profitable process [2, 5, 6]. The commonly used in the FTS or proposed for the SRE heterogeneous catalysts are cobalt-based ones [2–7], usually highly dispersed on inorganic oxide supports [8], which show a high activity and stability, relatively low cost and a high selectivity for the most desirable reaction products [9]. Among supports of the active phase, cerium oxide was used very often in various catalytic systems [3, 10, 11]. Ceria is characterized by a high oxygen transport and its storage capacity, by shifting between Ce^{3+} and Ce^{4+} under reductive-oxidative conditions [12, 13]. Due to these properties, cerium oxide shows a high affinity for H_2 and CO molecules [3], and thereby, an activity in various catalytic reactions such as water gas shift, oxidation of hydrocarbons or oxidation of CO [10, 13]. Ceria is also widely used in supported catalysts proposed to the SRE [14–16].

The catalytic properties of catalysts depend on their key parameters, such as crystallites size, structure and morphology [17]. Dispersion (and the average size) of the metallic active phase is one of the most important parameters characterizing the heterogeneous catalysts [8], which are essential for the activity, selectivity and stability of catalytic processes. The catalytic activity of a supported catalysts depends on the degree of dispersion of the metallic active phase and its active surface area [8, 18], and it usually increases with increasing dispersion of metal and decreasing its crystallites size [18]. On the other hand, the crystallites shape and their size distribution are important for mechanism of catalytic reaction, which dependents on the crystal faces exposed at the surface [19].

The crystallites size of metallic active phase are usually determined by hydrogen chemisorption, X-ray diffraction (XRD) or TEM (Transmission Electron Microscopy) [8, 17, 20–22], but sometimes different results are found from various methods for the same catalyst. The differences in measurements of the crystallites size can result from methods limitation. In the case of various active phases, limitations of the XRD measurements can result from the fact that XRD does not measure the smallest particles. The measurement limitations can also concern hydrogen adsorption capacity which can be diminished by strong metal-support interactions [9].

The evaluation of dispersion of the active phase, on the basis of hydrogen chemisorption data is a common, simple and cheap method. However, literature show that temperature of hydrogen chemisorption measurements can significantly influence on obtained results. More than 40 years ago Bartholomew et al. [23–25] show that the chemisorption of hydrogen over cobalt catalysts with various supports (SiO_2, Al_2O_3, C, MgO, ZSM-5, TiO_2) and over unsupported cobalt is activated and highly reversible. The activation was a function of the interaction of cobalt with a support or promoter. Frequently used in catalysis, potassium promoter significantly increased the adsorption activation energy for hydrogen [26]. It is also proved that some methods for determining the hydrogen uptake, i.e. flow adsorption methods such as thermal desorption and pulse methods, measure only irreversible (strong) chemisorption [23, 27]. No hydrogen desorption was detected for MgO- and ZSM-5-supported and low-loaded (1–3 wt.%) alumina-supported cobalt catalysts using TPD method, even though those catalysts adsorbed hydrogen when the static technique was applied [23, 24]. The special case is the Co/TiO_2 system, where due to the strong metal-support interactions the stoichiometry of hydrogen chemisorption is lower than one hydrogen atom per surface cobalt atom, even in static measurements. With exception of the cobalt systems in which the strong metal-support interactions take place, the static technique was recommended for estimation of the average size of cobalt crystallites on the basis of maximal hydrogen chemisorption uptake, usually at 373 K. A good correlation with TEM measurements was found for the Co/SiO_2, $Co/\gamma\text{-}Al_2O_3$ and Co/C catalysts. The paper [9] also shows that the volume of chemisorbed hydrogen (including strong and weak chemisorption) on the $CoRe/\gamma\text{-}Al_2O_3$ catalyst varies with the temperature of chemisorption, and the use of different data leads to the determination of different average size of crystallites, even though the actual crystallites size remains unchanged. They obtained the best results when the total chemisorption uptake measured at 373 K was used for cobalt dispersion calculation. In the current literature, there is a large discrepancy between conditions and a manner of hydrogen chemisorption measurements, from which data are used to determine the average size of crystallites and dispersion of the metallic cobalt phase deposited on an oxide support. Although those, already old, recommendations, only in the 2015-beginning of 2016 period the much lower temperature, 293–323 K, of hydrogen chemisorption [28–37] and flow adsorption pulse and TPD methods [32–37] are used in many laboratories. The higher, 423 K, temperature of hydrogen chemisorption was also applied in the pulse method for estimation of the average size of cobalt crystallites [33].

From three methods (hydrogen chemisorption, TEM and XRD) used for crystallites size determination, only TEM shows distinct advantages for the direct measurement of crystallites size in comparison with other methods, because the metal active phase crystallites can be quite clearly distinguished from the catalyst support and directly measured. Additionally to the crystallite diameters measurement, TEM

allows determining of crystallites size distribution and also to carry out morphological characteristics of crystallites, such as the shape and the structure [25].

The aim of this work is determination of the optimum temperature for hydrogen chemisorption and evaluation of correctness of the use of the total and strong chemisorption data to determine of the average size of cobalt-based active phase crystallites, supported on ceria. There was not previously shown whether, and to what extent, this support oxide, having a special previous mentioned properties, influences activation of hydrogen chemisorption and what the chemisorption temperature is necessary to obtain the average size of cobalt crystallites the most compatible with the crystallites size determined by the most objective transmission electron microscopy method (taking into account a statistically high number of crystallites measured). The influence of potassium promoter of ceria-supported cobalt-based catalyst on the optimal for this application hydrogen chemisorption temperature will be also determined. The results obtained by these two methods will be compared also with the values of the average size of crystallites obtained by the X-ray diffraction method.

Crystallites size of the cobalt-based active phase will be determined in the ceria-supported cobalt catalysts in which the active phase was promoted/unpromoted with 2 wt.% of potassium. Such catalysts are considered for the use in the SRE for production of hydrogen-rich gas for fuel cells fuelling.

2 Experimental

2.1 Catalyst Preparation

The Co/CeO_2 and KCo/CeO_2 catalysts were prepared by two-step impregnation of cerium oxide support. Prior to the impregnation ceria (Aldrich) was dried at 383 K for 3 h. For the first impregnation an aqueous solution of cobalt nitrate with citric acid CA (Co/CA = 1/1 mol/mol) were used. For the second impregnation, for the K-promoted catalyst an aqueous solution of potassium nitrate was used. After each impregnation, the catalyst precursor was dried at 383 K for 12 h, then calcined at 673 K with the heating rate of 2.2 K/min up to the calcination set point and maintained for 1 h at this temperature. Before all measurements the catalysts were reduced with hydrogen at 673 K for 1 h. The in situ XRD measurements confirmed complete reduction of cobalt oxide to metallic cobalt.

2.2 Hydrogen Chemisorption

Hydrogen adsorption isotherms were measured in a standard, commercial volumetric apparatus (Micromeritics, ASAP 2020C). The reactor was loaded with 0.9 g of the catalyst. Prior to the measurements, the catalysts were in-situ reduced in flowing hydrogen with the temperature programmed from ambient to 673 K with the heating rate of 10 K/min. The 673 K temperature was maintained for 1 h. After reduction, the samples were evacuated for 2 h at the reduction temperature. Then, under the vacuum of 3.8×10^{-7} Pa, the catalyst samples were cooled down to the temperature of chemisorption. Hydrogen chemisorption isotherms were measured in the range of 313–433 or 453 K and in the pressure range of 15–475 mmHg. Subsequently, the sample of catalyst was evacuated for 30 min, keeping the constant temperature (the same at which the first isotherm was taken), and the second isotherm of weak chemisorption was recorded. The strong chemisorption isotherm of hydrogen was calculated as a difference of the first (total) and the second (weak) isotherms. For measurements of the chemisorption isotherms at various temperatures always the new catalyst sample was used. The uptake of hydrogen (total, weak and strongly chemisorbed) was determined by extrapolating the straight-line portion of isotherms to zero pressure. The surface area of the cobalt active phase was calculated assuming a commonly used chemisorption stoichiometry Co:H = 1:1 [25, 27] and the surface area occupied by one atom of hydrogen equal to 0.065 nm [27]. The average size of cobalt crystallites was calculated assuming their spherical (or semi-spherical) shape, from the common Eq. (1):

$$d = 6 \cdot 10^3 / (d_{Co} \cdot S_{Co}) \quad (1)$$

where δ_{Co} is the density of cobalt (g/cm^3) and S_{Co} is the surface area of cobalt (m^2/g_{Co}).

2.3 TEM Measurements

The catalysts (fresh, oxide form) were grinded in an agate mortar to fine powders. The resulting powder of each catalyst was poured with 99.8 % ethanol (POCH) to form slurry which subsequently was inserted into a ultrasonic homogenizer for 20 s. Then, the catalyst-containing slurry was pipetted and supported on a 200 mesh copper grid covered with lacey formvar and stabilized with carbon (Ted Pella Company) and left on a filter paper for ethanol evaporation. The samples deposited on the grid were inserted to a single-tilt holder and moved to the electron microscope.

The catalysts reduced in a fixed-bed reactor with hydrogen flow rate of 100 ml/min at 673 K were transferred in a closed reactor to a glovebox. The reactor was opened and the catalyst was prepared for TEM measurements in the glovebox filled with argon (it protected the catalyst from oxidation), and applied to the copper grid covered with lacey formvar and stabilized with carbon. Next, the each catalyst deposited on the grid was inserted into the vacuum transfer holder (Gatan); the holder was closed and the catalyst was transferred in argon atmosphere to the microscope. The high-resolution electron microscope Titan G2 60–300 kV (FEI Company), equipped with: the field emission gun

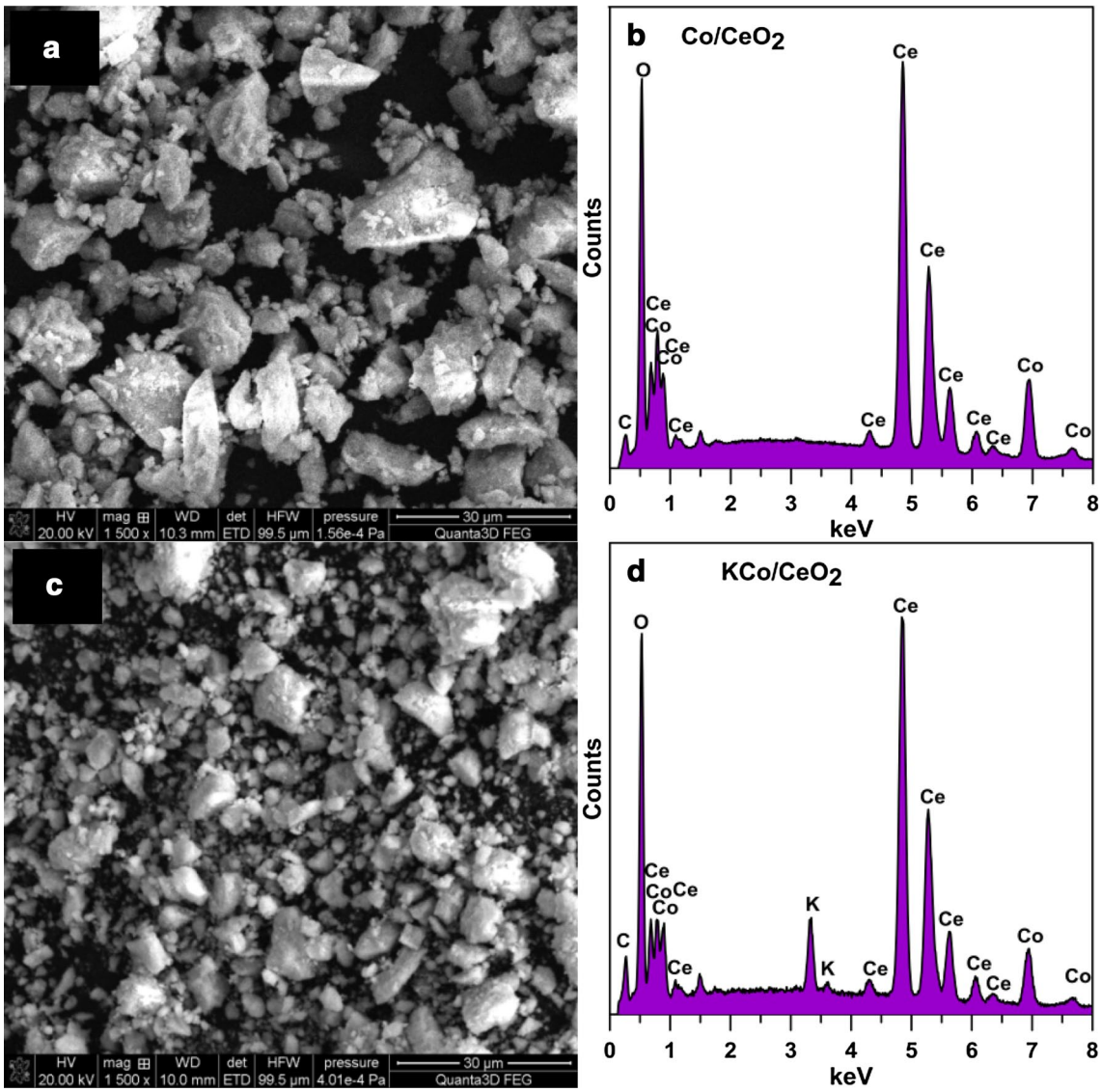

Fig. 1 SEM images and qualitative EDS spectra of (**a, b**) Co/CeO_2 and (**c, d**) KCo/CeO_2 catalysts

Table 1 Quantitative EDS analysis of main elements in Co/CeO_2 and KCo/CeO_2 catalysts

Element	Co/CeO_2		KCo/CeO_2	
	Wt.%	At.%	Wt.%	At.%
Co	9.44 ± 0.29	9.18 ± 0.24	8.83 ± 0.33	8.47 ± 0.86
K	–	–	2.16 ± 0.40	3.18 ± 0.47

(FEG), monochromator, three condenser lenses system, the objective lens system, image correction (C_s-corrector), HAADF detector and EDS spectrometer (Energy Dispersive X-ray Spectroscopy) was used to display the catalysts. Microscopic studies of the catalysts were carried out at an accelerating voltage of the electron beam equal to 300 kV for the catalysts in the oxide and reduced forms.

The elements mapping was carried out in the STEM mode by collecting point by point EDS spectrum of each of the corresponding pixels in the map. The collected maps were presented in the form of a matrix of colored pixels with the intensity corresponding to the amount of the element.

The size and shape of the particles in the fresh and reduced Co/CeO_2 and KCo/CeO_2 catalysts were determined by using the high resolution TEM (HRTEM) imaging and FFT. Phase separation (crystal lattice of the cerium oxide and crystal lattice of the active phase—for better distinguishing of support and active phase crystallites) was performed with the FFT by using a masking available in the Gatan DigitalMicrograph software package. On the basis of the FFT generated from HRTEM images of the fresh and reduced catalysts, individual phases with various crystallographic orientation derived from ceria support and as well

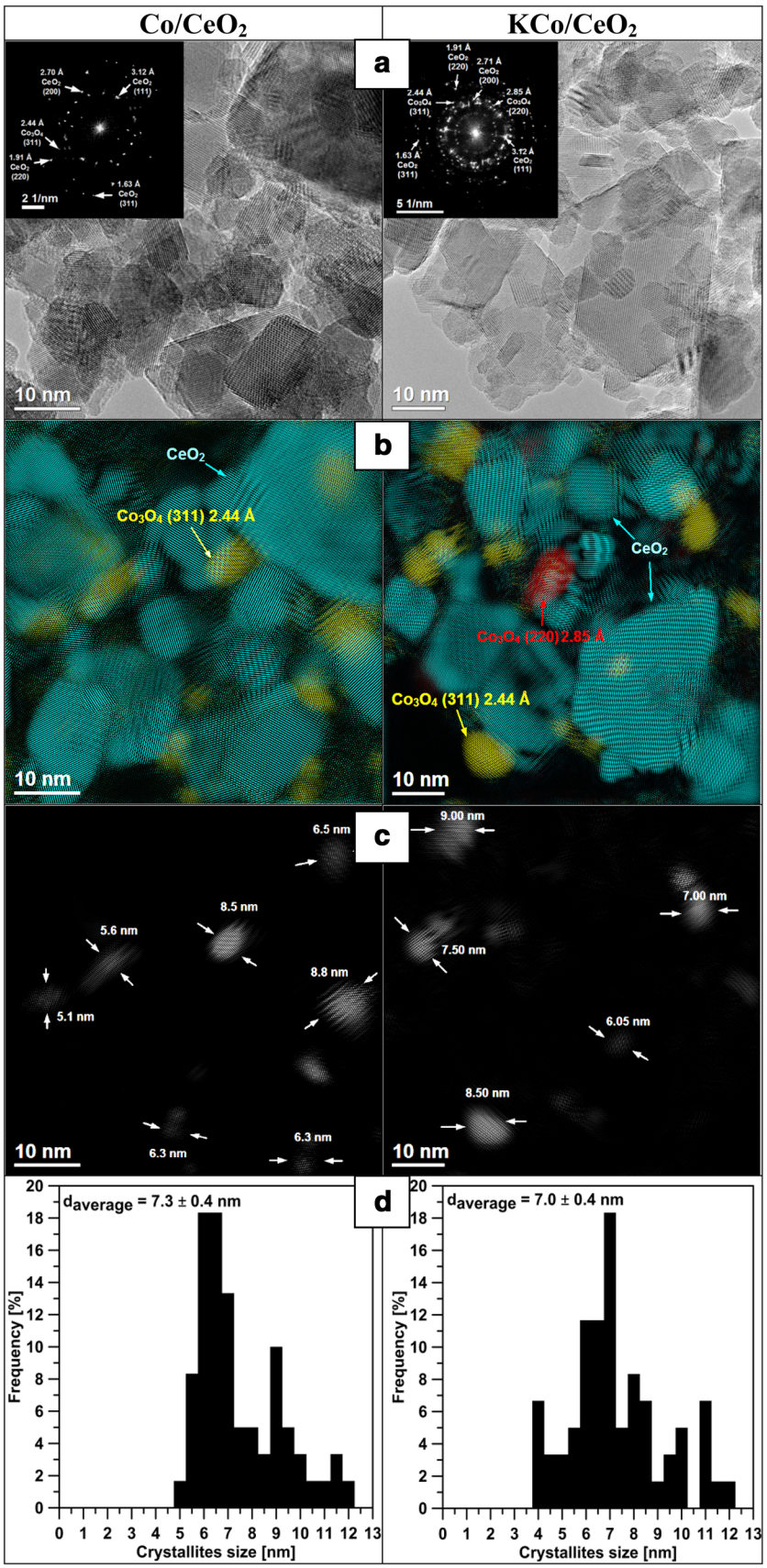

Fig. 2 **a** HRTEM images, **b** phase identification, **c** cobalt-based crystallites size measurements example and **d** cobalt-based crystallites size distributions in the fresh (in the oxide form) Co/CeO_2 and KCo/CeO_2 catalysts

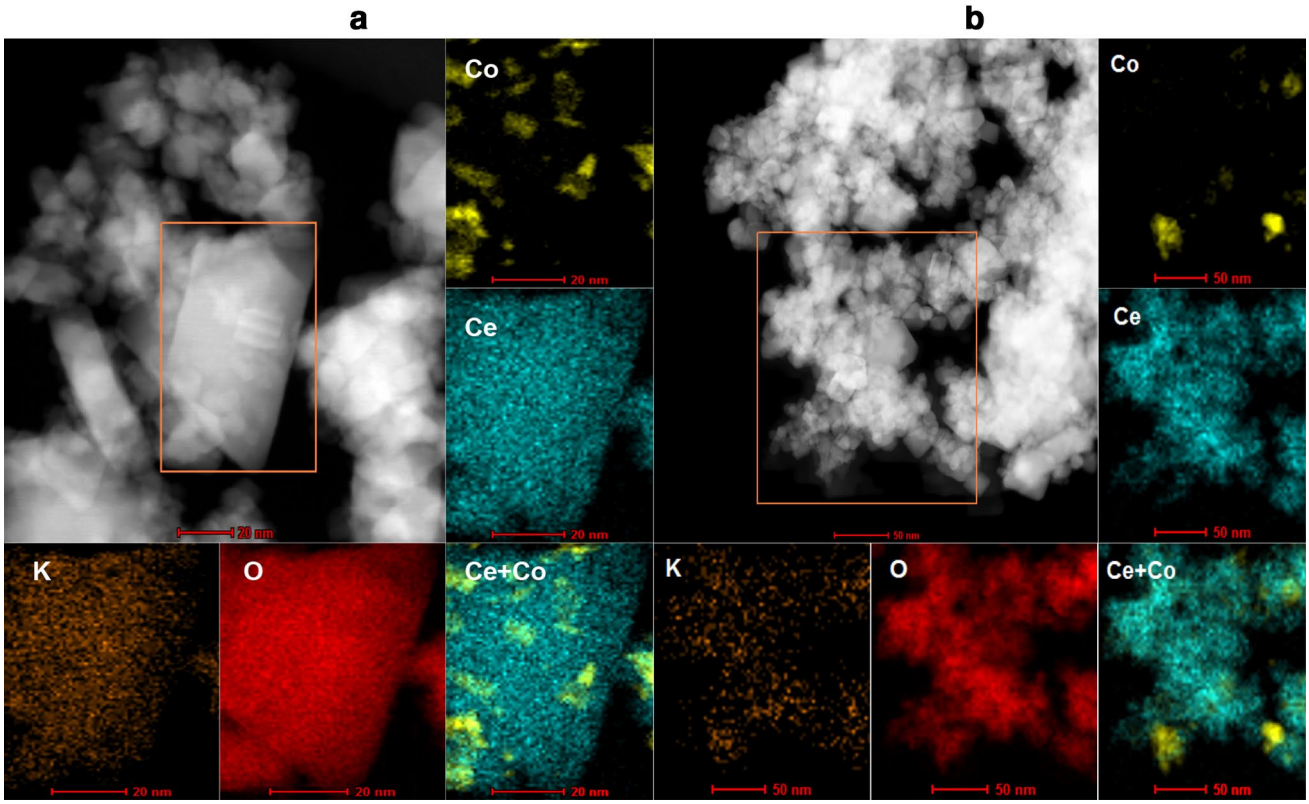

Fig. 3 STEM-EDS analysis of **a** the fresh (in the oxide form) and **b** the reduced KCo/CeO_2 catalyst

as active phase in various forms, Co_3O_4 (oxide) and Co^0 (reduced), respectively were identified. Then, the mask was imposed on the FFT in order to separate crystallites of the active phase (Co_3O_4 or Co^0) from crystallites of the support present on the HRTEM images. The measurements of the size of separated crystallites of the active phase allowed us to determine distribution of crystallites size. Particle size distribution was obtained by measuring diameter of about 150 particles for all TEM measurements. The average size of particles was then calculated from the Eq. (2):

$$d_{average} = \sum N_i D_i / \sum N_i \quad (2)$$

where: N_i—the numbers of metal crystallites in a specific size range, D_i—the average diameter in each diameter range.

Qualitative and quantitative contents of main elements in the catalysts were determined from EDS spectra collected by using the FEI Quanta 3D FEG scanning electron microscope, equipped with the EDS spectrometer.

2.4 XRD Measurements

Before XRD measurements, the catalysts were in-situ reduced at 673 K in hydrogen flow rate of 100 ml/min in the XRK 900 reactor chamber (Anton Paar). X-ray diffraction patterns were collected at two temperatures, at 303 K for the fresh (oxide) samples and at 673 K (reduced samples) with Empyrean (PANalytical) X-ray diffractometer, using CuKα radiation ($\lambda = 1.54 \times 10^{-10}$ m). The analyses were recorded in the 2θ range between 10° and 110°. For measurements at 303 K the average crystallites size of cobalt oxide was calculated from the Scherrer equation [38] using the Co_3O_4 (311) peak located at $2\theta = 36.8°$. The metallic cobalt particles size in reduced catalysts was also calculated from Scherrer formula using the Co (002) peak located at $2\theta = 44.3°$. A standard crystal of cerium oxide was used as a reference material for determination of the instrumental line broadening.

3 Results and Discussion

3.1 TEM Characterization of Fresh and Reduced Catalysts

Figure 1 shows SEM images of (a) Co/CeO_2 and (c) KCo/CeO_2 catalysts and qualitative EDS spectra (b and d, respectively), collected from the fresh (in oxide form) catalysts. In Table 1, the percentage of weight and the percentage of atomic contents of main elements in the catalysts obtained from EDS spectra, are shown. Based on quantitative data the following content of cobalt in the fresh Co/CeO_2 catalyst was

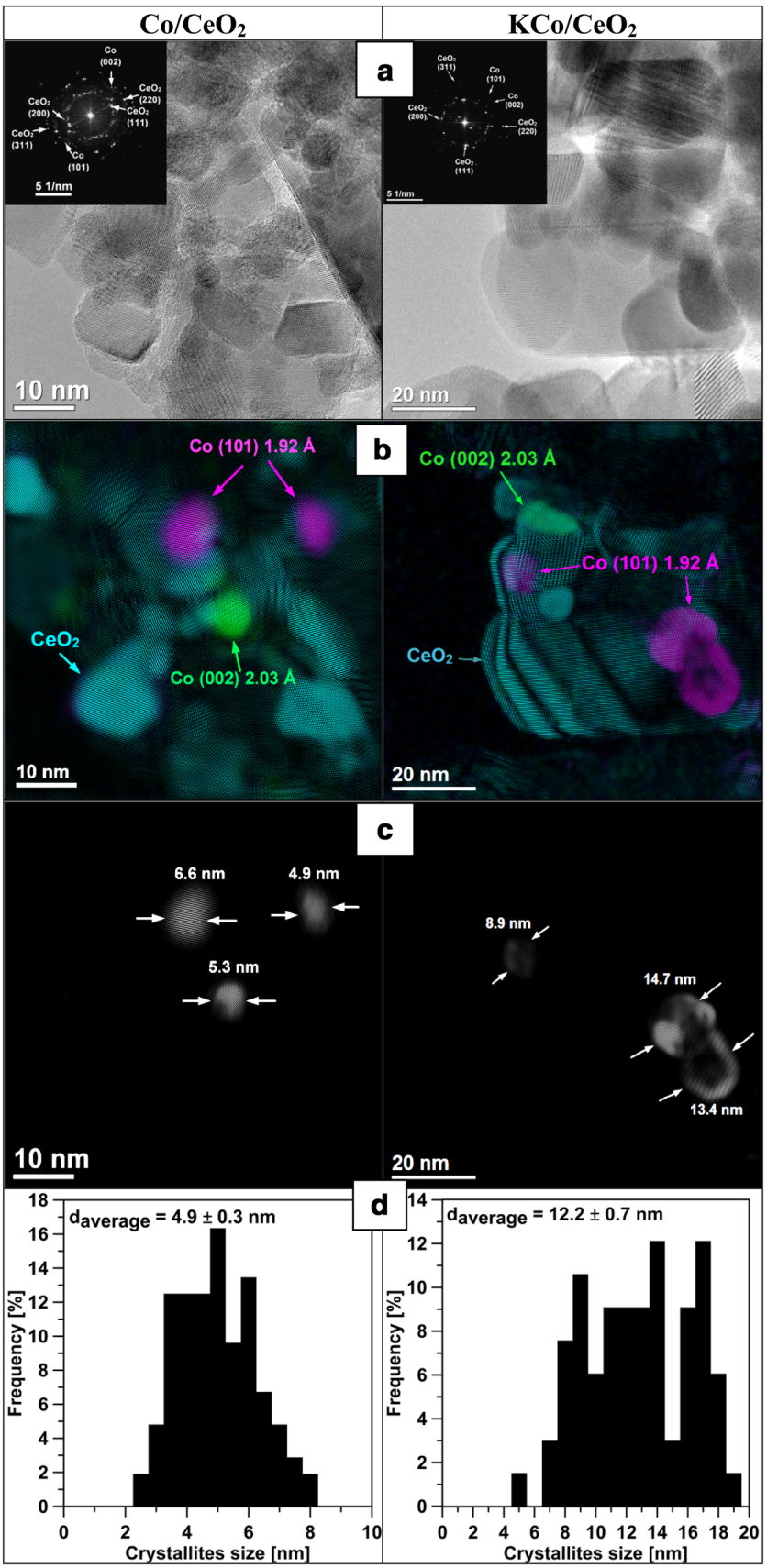

Fig. 4 **a** HRTEM images, **b** phase identification, **c** cobalt-based crystallites size measurements example and **d** cobalt-based crystallites size distributions in the reduced Co/CeO_2 and KCo/CeO_2 catalysts

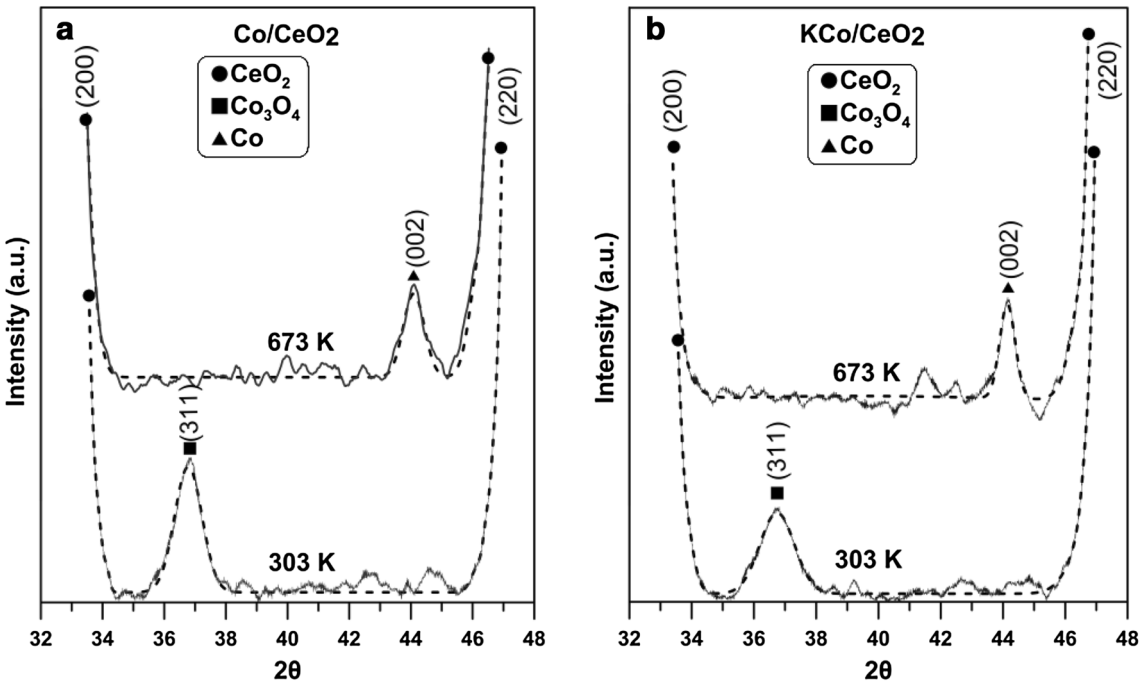

Fig. 5 XRD patterns of Co/CeO_2 and KCo/CeO_2 catalysts performed at 303 K (fresh, oxide form) and at 673 K after in situ reduction with hydrogen

Table 2 Comparison of the average size of crystallites determined by TEM, XRD and hydrogen chemisorption for fresh and reduced (at 673 K) Co/CeO_2 and KCo/CeO_2 catalysts

Catalyst	TEM (nm)		XRD (nm)		Hydrogen chemisorption (nm)
	Fresh	Reduced	Fresh	Reduced	
Co/CeO_2	7.3 ± 0.4	4.9 ± 0.3	7.4 ± 0.4	7.8 ± 0.4	4.1 ± 0.3*
KCo/CeO_2	7.0 ± 0.4	12.2 ± 0.7	7.1 ± 0.4	15.2 ± 0.8	12.5 ± 0.3**

Measured at *383K, **413K

determined: 9.44 ± 0.29 wt.%, and for the fresh KCo/CeO_2 catalyst the following contents of elements were determined: 8.94 ± 0.28 wt.% of cobalt and 1.93 ± 0.10 wt.% of potassium.

Among of the facets identified on the basis of the FFT in the fresh Co/CeO_2 and KCo/CeO_2 catalysts (Fig. 2), the facets originating from the CeO_2 support with interplanar distances 3.12, 2.70, 1.91, 1.63 Å and crystallographic orientations (111), (200), (220), (311) and the facets originating from the active phase in the oxide form (Co_3O_4) with interplanar distances 2.44, 2.85 Å and crystallographic orientations (311), (220) were found. The average crystallites size of the oxide cobalt-based active phase in the unpromoted fresh catalyst was 7.3 nm while in the K-promoted fresh catalyst this value was equal to 7.0 nm.

STEM-EDS analysis (Fig. 3a) shows a good dispersion of cobalt (Co, Ce + Co maps) and very good dispersion of potassium (K map) in the fresh KCo/CeO_2 catalyst. Similar dispersion of elements (not show here) was found in the K-unpromoted catalyst. Additionally, the EDS map of potassium indicates that it is dispersed both on cobalt and on ceria phases.

The same microscopic measurements were applied to determine phases present in both K-promoted and unpromoted catalysts in their reduced form (Fig. 4). The phase which originates from the support was identified as CeO_2 with interplanar distances 3.12, 2.70, 1.91 and 1.63 Å corresponding to the crystal planes (111), (200), (220) and (311), respectively. The cobalt active phase was found as Co^0 with interplanar distances 1.92 and 2.03 Å corresponding to the crystal planes (101) and (002), respectively. On the basis of the phases separation generated from the masking process, metallic cobalt was distinguished from the support and its crystallite size distributions was determined for both reduced catalysts. The average size of cobalt-based crystallites in the unpromoted reduced catalyst was 4.9 nm while in the K-promoted reduced catalyst this value was equal to 12.2 nm. The increase of crystallites size after reduction at 673 K (from 7.0 nm for the oxide form to 12.2 nm for the reduced form) was observed only for the catalyst promoted with potassium. It suggests that the addition of potassium favours sintering of Co crystallites. The reduction of the unpromoted catalyst caused decreasing of the crystallites size from 7.3 nm (oxide form) to 4.9 nm (reduced form). The ratio of the average crystallites size (d) of the active phase in reduced form (Co) to the oxidized form (Co_3O_4) is equal 0.7 for unpromoted catalyst. For K-promoted catalyst this ratio is equal 1.7.

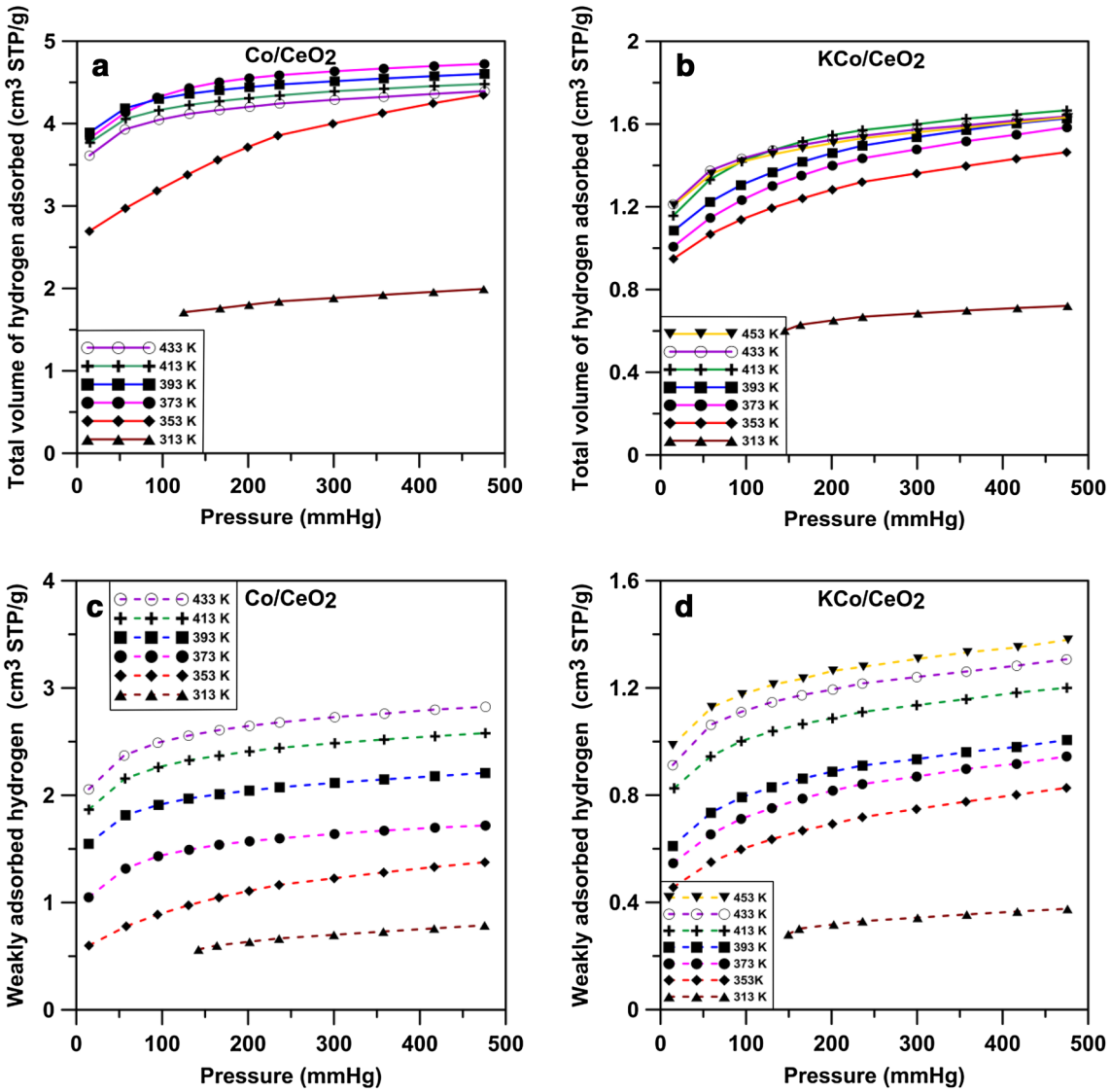

Fig. 6 Total (**a, b**) and weak (**c, d**) hydrogen chemisorption isotherms measured at various temperatures over Co/CeO_2 and KCo/CeO_2 catalysts pre-reduced in situ at 673 K

STEM-EDS analysis of reduced KCo/CeO_2 catalyst (Fig. 3b) shows good dispersion of metallic cobalt (Co, Ce + Co maps) and very good dispersion of potassium (K map). The comparison of cobalt distribution maps obtained for the fresh (Fig. 3a) and reduced (Fig. 3b) potassium-promoted catalysts confirms that the crystallites size of the active phase increases after reduction. In the case of unpromoted catalyst, the decreasing of the size of cobalt-based phase due to the reduction was also confirmed by STEM-EDS analysis (not show here).

3.2 X-ray Study of Crystallites Size

The crystallites sizes of the cobalt-based active phase determined on the basis of the X-ray measurements (Fig. 5) are presented in Table 2. Cobalt oxide crystallites sizes in both unpromoted and K-promoted catalysts are comparable with those determined on the basis of the TEM measurements. Also, the XRD studies showed that in the KCo/CeO_2 catalyst the crystallites size of the cobalt active phase in oxide form (Co_3O_4) is much smaller than the size of crystallites in metallic form (after hydrogen reduction at 673 K). An increase in the crystallites size of the active phase, from 7.1 nm for oxidized form Co_3O_4 to 15.2 nm—for metallic cobalt form, was observed. Whereas, for the unpromoted catalyst (Co/CeO_2) such significant change in the size of crystallites was not seen (oxide form 7.4 nm, reduced form 7.8 nm).

The analysis of X-ray diffraction data is known as a simple and rapid, however the results obtained for reduced catalysts were in contrast to those obtained from TEM measurements and the determined size of crystallites was not

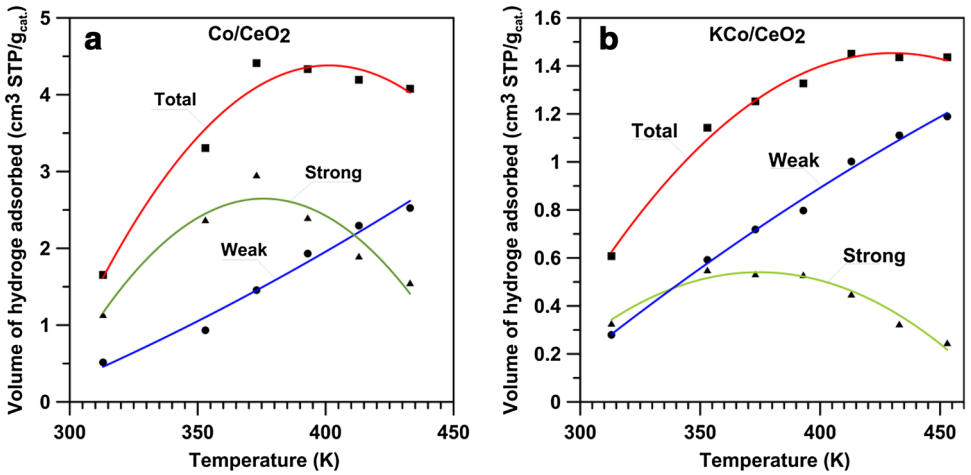

Fig. 7 Total, weak and strong hydrogen chemisorption over **a** Co/CeO_2 and **b** KCo/CeO_2 catalysts, measured at various temperatures

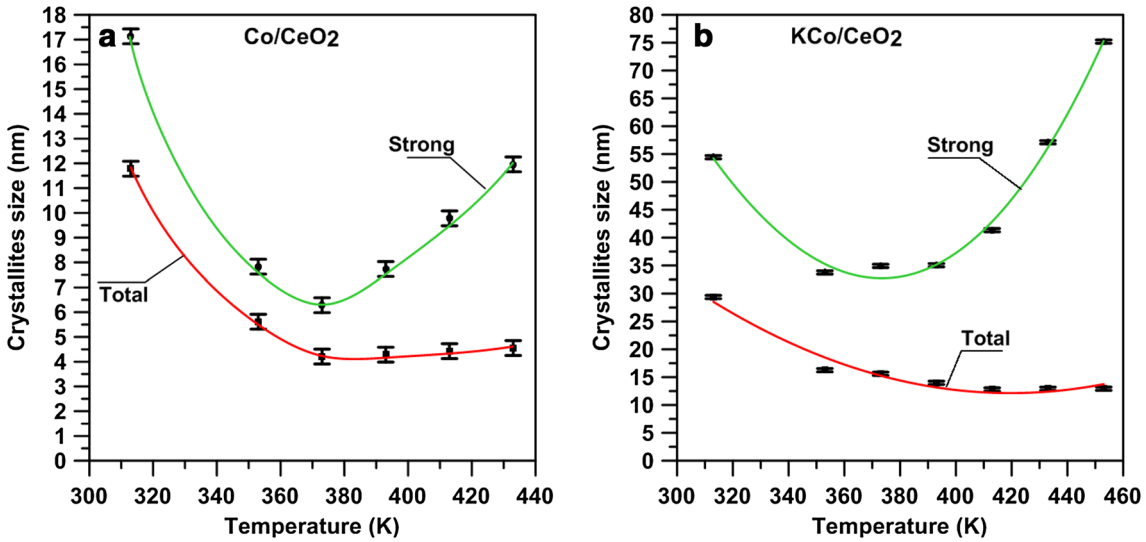

Fig. 8 Calculated average crystallites size of the Co active phase determined (calculated) from the total and strong hydrogen chemisorption data obtained at various temperatures for **a** Co/CeO_2 and **b** KCo/CeO_2 catalysts

very accurate. This incompatibility may results from inherent limitations in the peak profile analysis of the XRD data with the use of a width of the peak at the half of its maximum, what excludes very small crystallites from XRD data analysis [25].

3.3 Hydrogen Chemisorption Studies

Figure 6 shows the total and weak hydrogen chemisorption isotherms on the Co/CeO_2 and KCo/CeO_2 catalysts pre-reduced in-situ at 673 K and measured in the range of the temperature from 313 to 433 or 453 K. With the increased temperature the isotherms become linear at lower equilibrium pressures for both samples and the amount of chemisorbed hydrogen initially increases, then goes through a maximum and finally it decreases a little at the highest temperatures. There were two adsorption isotherms recorded in each experiment, the first one includes the total hydrogen adsorption and the second one includes only weak hydrogen adsorption. The difference between these two adsorption isotherms indicates the amount of a strong hydrogen adsorption on the cobalt catalysts [39].

The amounts of the total and weak hydrogen chemisorbed and the difference between total chemisorption and weak chemisorption, i.e. hydrogen strongly chemisorbed, at each measurement temperature, for both catalysts are presented in Fig. 7. For both catalysts, in the lower temperatures range the increase of the temperature causes simultaneously increase of the total, weak and strong chemisorption. The maximum of the total chemisorption was obtained at 383 K for the Co/CeO_2 catalyst and at 413 K in the case of KCo/CeO_2 catalyst. In the case of the strong

chemisorption the maximum of hydrogen uptake was at 373 K for both samples. Above the temperature of maxima of hydrogen chemisorption a small decline of the total and very clear decline of strongly adsorbed hydrogen amounts were observed. In the whole range of temperatures, weak chemisorption increased almost linearly.

Figure 8 shows the average crystallites size of metal active phase determined (calculated) on the basis of the total and strong chemisorption for Co/CeO_2 and KCo/CeO_2 catalysts. The lowest crystallites size of 6.5 nm for the Co/CeO_2 catalyst and 34 nm for the KCo/CeO_2 catalyst was determined from the strongly chemisorbed hydrogen uptake at 373 K. Below and above this chemisorption temperature the calculated crystallites sizes are much larger. In the case of the total amount of chemisorbed hydrogen, the lowest average size of cobalt-based crystallites in the unpromoted Co/CeO_2 catalyst, i.e. 4.1 nm, was calculated using the hydrogen chemisorption uptake obtained at 383 K. For the potassium-promoted KCo/CeO_2 catalyst, the smallest average size of cobalt crystallites was determined from the total chemisorption of hydrogen data obtained at 413 K. Using the total hydrogen uptake from lower temperatures the calculated average crystallites size is much higher. Above indicated temperatures of chemisorption the calculated crystallites size does not differ significantly from those obtained from maximum hydrogen uptake data. The hydrogen chemisorption studies show also that in the case of the catalyst promoted with potassium the higher temperature of hydrogen chemisorption is required to obtain the smallest crystallites size of the cobalt-based active phase.

Our comparative studies on determination of cobalt crystallites size by various methods, such as TEM, XRD and hydrogen chemisorption, show a very good correlation of results obtained with TEM and hydrogen chemisorption methods, when the total hydrogen chemisorption data obtained at 383 K (or at 413 K when the catalyst is promoted with potassium) are used for determination of the dispersion of cobalt-based active phase (Table 2).

Such temperature conditions used for hydrogen chemisorption and the total hydrogen uptake should be used for determination of the average size of cobalt-based crystallites by using of hydrogen chemisorption data. Because the difference in the size of crystallites in the unpromoted and K-promoted catalysts estimated from the hydrogen chemisorption data obtained at 383 and 413 K is very small (Fig. 8) for routine studies of large number of potassium-free and potassium-promoted catalysts, the chemisorption temperature from the range of 383–413 K may be also acceptable. Our results also clearly prove that the average size of cobalt crystallites determined from strongly chemisorbed hydrogen uptake is overestimated. This may be also the case of the flow adsorption methods, i.e. the pulse adsorption or the temperature-programmed desorption methods, where weakly chemisorbed hydrogen is removed from the metal surface by an inert gas before desorption measurements.

4 Conclusions

Comparison of the average size of the cobalt-based crystallites measured by TEM, hydrogen chemisorption and XRD methods proved that the good agreement between values obtained from total chemisorption and TEM data is possible. The total hydrogen uptake on the potassium-free catalyst, measured at 383 K, leads to the estimation of the size of crystallites compatible with the values measured by the most objective, microscopic method. When potassium is present in the catalyst, the optimum of hydrogen chemisorption temperature is higher by c.a. 30 K, i.e. 413 K.

The average size of cobalt-based crystallites estimated from XRD data is congruous with that measured by the TEM method only in the case when among crystallites there are no very small ones.

Acknowledgments The research was carried out with the equipment purchased thanks to the financial support of the European Regional Development Fund in the framework of the Polish Innovation Economy Operational Program (contract no. POIG.02.01.00-06-024/09 Centre for Functional Nanomaterials; http://www.cnf.umcs.lublin.pl). All measurements presented in this article were done in the Analytical Laboratory of the Chemistry Faculty at the University of Maria Curie-Sklodowska accredited according to the ISO/IEC 17025:2005 international standard by the Polish Centre for Accreditation.

References

1. Zhou W, Wachs IE, Kiely ChJ (2012) Curr Opin Struct 16:10
2. Ni M, Leung DYC, Leung MKH (2007) Int J Hydrog Energy 32:3238
3. Arsalanfar M, Mirzaei AA, Bozorgzadeh HR, Atashi H, Shahriari S, Pourdolat A (2012) J Nat Gas Sci Eng 9:119
4. Spadaro L, Arena F, Granados ML, Ojeda M, Fierro JLG, Frusteri F (2005) J Catal 234:451
5. Rybak P, Tomaszewska B, Machocki A, Grzegorczyk W, Denis A (2011) Catal Today 176:14
6. Khodakov AY, Chu W, Fongarland P (2007) Chem Rev 107:1692
7. Figen HE, Baykara SZ (2015) Int J Hydrog Energy 40:7439
8. Borodziński A, Bonarowska M (1997) Langmuir 13:5613
9. Xiong J, Borg Ø, Blekkan EA, Holmen A (2008) Catal Commun 9:2327
10. Namai Y, Fukui K, Iwasawa Y (2003) J Phys Chem B 107:11666

11. Al-Hmoud L, Jones ChW (2013) J Catal 301:116
12. Trovarelli A, Zamar F, Llorca J, de Leitenburg C, Dolcetti G, Kiss JT (1997) J Catal 169:490
13. Lin SS-Y, Kim DH, Ha SY (2009) Appl Catal A 355:69
14. Zanchet D, Santos JBO, Damyanova S, Gallo JMR, Bueno JMC (2015) ACS Catal 5:3841
15. Haryanto A, Fernando S, Murali N, Adhikari S (2005) Energy Fuel 19:2098
16. Mattos LV, Jacobs G, Davis BH, Noronha FB (2012) Chem Rev 112:4094
17. Wang H, Wang C, Yan H, Yi H, Lu J (2015) J Catal 324:59
18. Carter JL, Cusumano JA, Sinfelt JH (1966) J Phys Chem 70:2257
19. Kępiński L (2010) Ann Univ M. Curie-Sklodowska, LXV, 2, Sect. AA: 9.
20. Kugai J, Fox EB, Song C (2015) Appl Catal A 497:31
21. Jianga X, Koizumi N, Guo X, Song Ch (2015) Appl Catal B 170–171:173
22. Aramendia MA, Borau V, Jiménez C, Marinas JM, Moreno A (1996) Colloids Surfaces A Physicochem Eng Aspects 106:161
23. Zowtiak JM, Weatherbee GD, Bartholomew CH (1983) J Catal 82:230
24. Zowtiak JM, Bartholomew CH (1983) J Catal 83:107.
25. Reuel RC, Bartholomew CH (1984) J Catal 85:63.
26. Bartholomew CH (1990) Catal Lett 7:27
27. Bergeret G, Gallezot P (2008) In: Ertl G, Knözinger H, Schüth F, Weitkamp J (eds) Handbook of heterogeneous catalysis. Wiley-VCH, Weinheim
28. Greluk M, Rybak P, Słowik G, Rotko M, Machocki A (2015) Catal Today 242:50
29. Banach B, Machocki A (2015) Appl Catal A 505:173
30. Yang J, Frøseth V, Chena D, Holmen A (2016) Surf Sci 648:67
31. Barrientosa J, Montes V (2015) Catal Today doi:10.1016/j.cattod.2015.10.039.
32. Wu H, Yang Y, Suo H, Qing M, Yan L, Wu B, Xu J, Xiang H, Li Y (2015) J Mol Catal A Chem 396:108
33. Rekha V, Sumana C, Douglas SP, Lingaiah N (2015) Appl Catal A 491:155
34. Zhao X, Lu G (2016) Int J Hydrog Energy 41:3349
35. Jian-Kang H, Li-Tao J, Bo H, De-Bao L, Yan L, Ya-Chun L (2015) J Fuel Chem Technol 43:846
36. Shimura K, Miyazawa T, Hanaoka T, Hirata S (2015) Appl Catal A 494:1
37. Sukkathanyawat H, Tungkamani S, Phongaksorn M, Rattana T, Narataruksa P, Yoosuk B (2015) Energy Procedia 79:372
38. Cullity BD (1978) Elements of X-ray diffraction. Addison-Wesley, London
39. Hilmen AM, Schanke D, Hanssen KF, Holmen A (1999) Appl Catal A 186:169